Nonlinear Bending Analysis of Thick Functionally Graded Plates Based on Third-Order Shear Deformation Plate Theory

P. Naderpour *
Department of Mechanical Engineering,
Najafabad Branch, Islamic Azad University, Isfahan, Iran
E-mail: peyman.naderpour@yahoo.com
*Corresponding author

A. Ghassemi & N. Solhjoei
Department of Mechanical Engineering,
Najafabad Branch, Islamic Azad University, Isfahan, Iran
E-mail: a_ghassemi@pmc.iaun.ac.ir , Solhjoei@yahoo.com

Received: 9 October 2013, Revised: 4 November 2013, Accepted: 8 December 2013

Abstract: The nonlinear bending analysis of thick functionally graded plates subjected to mechanical loading is studied in this paper. The formulation was derived based on the third-order shear deformation plate theory and Von Kármán type non-linearity. Young's modulus is assumed to vary according to the power law distribution in terms of the volume fractions of the constituents. The principle of virtual work was used to obtain the weak form of the governing differential equations. The most important advantage of employed numerical solution in this work is that the whole plate was considered as one element and the components of displacement field were interpolated over the entire domain, then a hierarchical finite-element scheme was developed. The validity and accuracy of the method was verified by comparisons made with other solutions. In addition, the effect of numbers of interpolation functions on the accuracy of results was studied. It is concluded that accurate results are obtained even by few numbers of interpolation functions.

Keywords: Functionally Graded Plates, Hierarchical Finite-Element Method, Nonlinear Bending, Third-Order Shear Deformation Plate Theory, Von Kármán Type Non-Linearity

Reference: Naderpour, P., Ghassemi, A., and Solhjoei, N., "Nonlinear Bending Analysis of Thick Functionally Graded Plates Based on Third-Order Shear Deformation Plate Theory", Int J of Advanced Design and Manufacturing Technology, Vol. 7/ No. 2, 2014, pp. 99-106.

Biographical notes: P. Naderpour is Master student of Mechanical Engineering at IAU, Njafabad branch, Isfahan, Iran. His current research interest includes Large Deformation Analysis of Plates and Shells. **A. Ghassemi** is Assistant Professor in Mechanical Engineering Department at the University of Najafabad, Iran. She received her PhD in Mechanical Engineering from Isfahan University of Technology, Iran. Her current research focuses on Damage, Constitutive Equations for Nanocomposites and Smart Materials. **N. Solhjoei** is Assistant Professor in Mechanical Engineering Department at the University of Najafabad, Iran. He received his PhD in Mechanical Engineering from University of Pierre and Marie Curie, France. His current research focuses on Computational Mechanics, Forming, Manufacturing and Vibrational Analysis.

1 INTRODUCTION

Functionally graded materials (FGMs) have received considerable research efforts, recently. That is why application of FGMs in variety of industries is growing significantly. Compared with the laminated composites, FGMs are inhomogeneous whose material properties vary continuously from one surface to another, which leads to elimination of interface problems and mitigation of thermal stress concentrations. Apart from much research conducted over the past years on FGMs fabrication, recently, solution of functionally graded (FG) plates subjected to small and large deformation has drawn much attention.

For analysis of plates the following theories were employed:

1. Classical plate theory
2. First-order shear deformation plate theories
3. Higher-order shear deformation plate theories such as REDDY's third-order theory [1], [2]

Since the classical plate theory, based on the Kirchhoff hypothesis, neglects the effects of transverse shear and normal strains, it is inaccurate for analyzing the distribution of displacements and stresses in thick plates with moderately large deformation. Therefore; a number of first-order shear deformation plate theories have been developed for taking into account these effects. Since in these theories the transverse shear strains are assumed to be constant through the thickness, shear correction factors have to be incorporated to adjust the transverse shear stiffness. The accuracy of the first-order shear deformation plate theory will be dependent on predicting better estimates for the shear correction factors. It has been shown that the classical and first-order shear deformation plate theories are inadequate to predict the accurate results for FG plates. Several refined higher-order plate theories that include the effects of transverse shear strains have been proposed. In third-order shear deformation plate theory proposed by REDDY the transverse shear strains are assumed to be parabolically distributed through the thickness of plate; hence, there is no need for shear correction factors [1], [2].

The solution of FG plates has been carried out both analytically and numerically. Cheng and Batra established an exact relationship between deflections of a simply supported functionally graded polygonal plate governed by either the third-order shear deformation theory or the first-order one and that of an equivalent homogeneous Kirchhoff plate [3]. Woo and Meguid proposed an analytical solution obtained in terms of Fourier series for the large deflection of functionally graded plates and shallow shells under transverse mechanical loading and a temperature field using Von Kármán theory [4].

Ma and Wang related the solution of the axisymmetric bending and buckling of functionally graded circular plates based on third-order plate theory (TPT) to those of isotropic circular plates based on classical plate theory (CPT) [5]. In addition, they studied effects of the gradient of material property and shear deformation on the axisymmetric bending and buckling of functionally graded plates according to first-order plate theory (FPT) and third-order plate theory, and comparisons of the TPT solutions with the FPT and CPT solutions were presented.

Chi and Chung studied a simply supported elastic rectangular FG plate subjected to transverse loads [6]. The material properties were assumed to vary continuously through the thickness, according to the volume fraction of the constituents based on power-law, sigmoid, and exponential functions. The classical plate theory and Fourier series expansion were employed to reach the series solutions. Nosier and Fallah reformulated the governing equations of the first-order shear deformation plate theory for FG circular plates into those describing the interior and edge-zone problems [7]. Then, they presented analytical solutions for axisymmetric and asymmetric behavior of isotropic FG circular plates within various boundary conditions under mechanical and thermal loadings.

Bo, et al. extended the method proposed by Mian and Spencer in order to consider an orthotropic FG plate subjected to uniform loading applied on the top surface [8], [9]. Then, they put forward elasticity solutions for an FG rectangular plate in cylindrical bending. Matsunaga presented a two-dimensional higher-order deformation theory for analysis of displacements and stresses in FG plates subjected to thermal and mechanical loadings [10]. He derived a set of fundamental governing equations which can take into account the effects of both transverse shear and normal stresses through the principle of virtual work using the method of power series expansion of continuous displacement components.

Mechab, et al. presented the bending analysis of FG plates using a two-variable refined plate theory, and Navier solution was used to obtain closed-form solutions for simply supported FG plates [11]. Suresh Kumar, et al., investigated nonlinear bending behavior of functionally graded plates according to higher-order theory [12]. The nonlinear simultaneous equations were obtained using Navier's method.

Fereidoon, et al., employed the differential quadrature (DQ) method for analyzing the isotropic functionally graded (FG) and functionally graded coated (FGC) thin plates [13]. They studied, then, the applicability of polynomial and harmonic differential quadrature (PDQ and HDQ) methods for bending analysis of these plates accurately under the transverse loading .The classical

thin plate theory was considered for the analysis. Woodward and Kashtalyan studied bending of an isotropic FG plate under localized transverse load by combination of 3-D analytical and computational (finite element) methods [14].

The aim of the current paper is to investigate the nonlinear bending behavior and static characteristics of FG plates subjected to mechanical loadings for two kinds of boundary conditions. The third-order shear deformation plate theory was employed to take into account the transverse shear strains, and the Von Kármán-type nonlinear strain-displacement relationship was adopted.

The principle of virtual work was used to obtain the weak form of the governing differential equations. The most important advantage of employed numerical solution in this work is that the whole plate was considered as one element and the components of displacement field were interpolated over the entire domain, then a hierarchical finite-element scheme was developed. To evaluate the accuracy of the method, the present results were compared with those of other researches. Studying the effect of numbers of interpolation functions on the results revealed that reaching the accurate results is possible even by few numbers of interpolation functions.

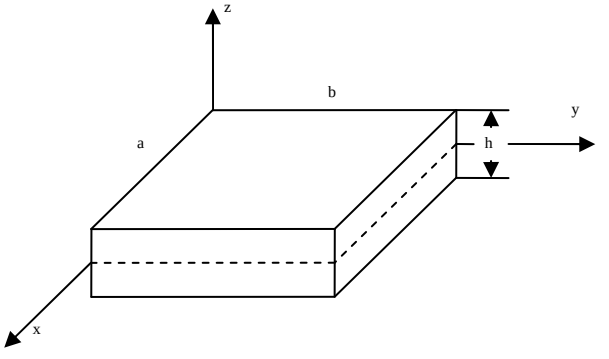

Fig. 1 Geometry of plate

2 Kinematics and constitutive equations

Consider a rectangular plate of length a, width b, and thickness h (Fig. 1). The origin of the coordinate system is located at the corner of the mid-plane at which displacements in x, y and z directions are $\bar{u}$, $\bar{v}$ and $\bar{w}$. $\bar{\psi}_x$ and $\bar{\psi}_y$ are defined as the mid-plane rotations of the normal about the y and x axes, respectively. According to REDDY's third-order shear deformation plate theory [1], [2], the displacement components are assumed to be of the following forms [15]:

$$u(x,y,z)=\bar{u}(x,y)+z\left[\bar{\psi}_x(x,y)-\frac{4}{3}\left(\frac{z}{h}\right)^2\left(\bar{\psi}_x(x,y)+\frac{\partial\bar{w}}{\partial x}\right)\right]$$
$$v(x,y,z)=\bar{v}(x,y)+z\left[\bar{\psi}_y(x,y)-\frac{4}{3}\left(\frac{z}{h}\right)^2\left(\bar{\psi}_y(x,y)+\frac{\partial\bar{w}}{\partial y}\right)\right]$$
$$w(x,y,z)=\bar{w}(x,y) \tag{1}$$

The strains of the plate related to the displacement field given in Eq. (1) are:

$$\varepsilon_1=\varepsilon_1^0+z(\kappa_1^0+z^2\kappa_1^2),\ \varepsilon_2=\varepsilon_2^0+z(\kappa_2^0+z^2\kappa_2^2),\ \varepsilon_3=0$$
$$\varepsilon_4=\varepsilon_4^0+z^2\kappa_4^2,\ \varepsilon_5=\varepsilon_5^0+z^2\kappa_5^2,\ \varepsilon_6=\varepsilon_6^0+z(\kappa_6^0+z^2\kappa_6^2) \tag{2}$$

Where:

$$\varepsilon_1^0=\frac{\partial\bar{u}}{\partial x}+\frac{1}{2}\left(\frac{\partial\bar{w}}{\partial x}\right)^2,\ \varepsilon_2^0=\frac{\partial\bar{v}}{\partial y}+\frac{1}{2}\left(\frac{\partial\bar{w}}{\partial y}\right)^2,\ \varepsilon_4^0=\bar{\psi}_y+\frac{\partial\bar{w}}{\partial y}$$
$$\varepsilon_5^0=\bar{\psi}_x+\frac{\partial\bar{w}}{\partial x},\ \varepsilon_6^0=\frac{\partial\bar{u}}{\partial y}+\frac{\partial\bar{v}}{\partial x}+\frac{\partial\bar{w}}{\partial x}\frac{\partial\bar{w}}{\partial y}$$
$$\kappa_1^0=\frac{\partial\bar{\psi}_x}{\partial x},\ \kappa_2^0=\frac{\partial\bar{\psi}_y}{\partial y},\ \kappa_6^0=\frac{\partial\bar{\psi}_x}{\partial y}+\frac{\partial\bar{\psi}_y}{\partial x}$$
$$\kappa_1^2=-\frac{4}{3h^2}\left(\frac{\partial\bar{\psi}_x}{\partial x}+\frac{\partial^2\bar{w}}{\partial x^2}\right),\ \kappa_2^2=-\frac{4}{3h^2}\left(\frac{\partial\bar{\psi}_y}{\partial y}+\frac{\partial^2\bar{w}}{\partial y^2}\right) \tag{3}$$
$$\kappa_4^2=-\frac{4}{h^2}\left(\bar{\psi}_y+\frac{\partial\bar{w}}{\partial y}\right),\ \kappa_5^2=-\frac{4}{h^2}\left(\bar{\psi}_x+\frac{\partial\bar{w}}{\partial x}\right)$$
$$\kappa_6^2=-\frac{4}{3h^2}\left(\frac{\partial\bar{\psi}_x}{\partial y}+\frac{\partial\bar{\psi}_y}{\partial x}+2\frac{\partial^2\bar{w}}{\partial x\partial y}\right)$$

The stress constitutive equations may be written as:

$$\begin{Bmatrix}\sigma_1\\ \sigma_2\\ \sigma_6\end{Bmatrix}=\begin{bmatrix}Q_{11} & Q_{12} & 0\\ Q_{21} & Q_{22} & 0\\ 0 & 0 & Q_{66}\end{bmatrix}\begin{Bmatrix}\varepsilon_1\\ \varepsilon_2\\ \varepsilon_6\end{Bmatrix}$$
$$\begin{Bmatrix}\sigma_4\\ \sigma_5\end{Bmatrix}=\begin{bmatrix}Q_{44} & 0\\ 0 & Q_{55}\end{bmatrix}\begin{Bmatrix}\varepsilon_4\\ \varepsilon_5\end{Bmatrix} \tag{4}$$

For FG plates Q_{ij} are given by:

$$Q_{11}=Q_{22}=\frac{E(z)}{1-\nu^2},\ Q_{12}=Q_{21}=\frac{\nu E(z)}{1-\nu^2}$$
$$Q_{16}=Q_{26}=Q_{61}=Q_{62}=Q_{45}=Q_{54}=0,\ Q_{44}=Q_{55}=Q_{66}=\frac{E(z)}{2(1+\nu)} \tag{5}$$

In the above equation, Young's modulus is assumed to vary through the thickness according to the following power law distribution.

$$E(z)=\left(E_c-E_m\right)\left(\frac{1}{2}+\frac{z}{h}\right)^n+E_m \tag{6}$$

for $(0\le n\le\infty)$

Where n is the power law index, h is the plate thickness, and E_c, E_m are the Young's modulus of the ceramic and the metal, respectively. The stress resultants and couple stresses are given by:

$$\begin{aligned}&(\overline{N}_i,\overline{M}_i,\overline{P}_i)=\int_{-h/2}^{+h/2}\sigma_i(1,z,z^3)\,dz \qquad i=1,2,6\\&(\overline{Q}_2,\overline{R}_2)=\int_{-h/2}^{+h/2}\sigma_4(1,z^2)\,dz,\quad(\overline{Q}_1,\overline{R}_1)=\int_{-h/2}^{+h/2}\sigma_5(1,z^2)\,dz\end{aligned} \tag{7}$$

Where $\overline{N}_i$ and $\overline{Q}_i$ are the membrane and transverse shear forces, $\overline{M}_i$ is the moment, and $\overline{P}_i$ and $\overline{R}_i$ are the higher-order moment and shear force, respectively. The constitutive relations of the plate can be yielded through substituting Eq. (4) into Eq. (7), and taking Eq. (2) into account.

$$\begin{aligned}&\begin{Bmatrix}\overline{\mathbf{N}}\\ \overline{\mathbf{M}}\\ \overline{\mathbf{P}}\end{Bmatrix}=\begin{bmatrix}\mathbf{A}&\mathbf{B}&\mathbf{E}\\ \mathbf{B}&\mathbf{D}&\mathbf{F}\\ \mathbf{E}&\mathbf{F}&\mathbf{H}\end{bmatrix}\begin{Bmatrix}\boldsymbol{\varepsilon}^0\\ \boldsymbol{\kappa}^0\\ \boldsymbol{\kappa}^2\end{Bmatrix}\\&\begin{Bmatrix}\overline{\mathbf{Q}}\\ \overline{\mathbf{R}}\end{Bmatrix}=\begin{bmatrix}\mathbf{A}&\mathbf{D}\\ \mathbf{D}&\mathbf{F}\end{bmatrix}\begin{Bmatrix}\boldsymbol{\varepsilon}^0\\ \boldsymbol{\kappa}^2\end{Bmatrix}\end{aligned} \tag{8}$$

Where $A_{ij,}\,B_{ij}$ etc., are the plate stiffnesses, given by:

$$\begin{aligned}&(A_{ij},B_{ij},D_{ij},E_{ij},F_{ij},H_{ij})=\int_{-h/2}^{+h/2}(Q_{ij})(1,z,z^2,z^3,z^4,z^6)\,dz\quad i,j=1,2,6\\&(A_{ij},D_{ij},F_{ij})=\int_{-h/2}^{+h/2}(Q_{ij})(1,z^2,z^4)\,dz\qquad\qquad i,j=4,5\end{aligned} \tag{9}$$

3 NUMERICAL SOLUTION SCHEME

For any point on the mid-plane, five degrees of freedom defined as components of displacement and rotation vector which are considered in matrix $\mathbf{U}$:

$$\mathbf{U}=\begin{Bmatrix}\overline{u}(x,y)\\ \overline{v}(x,y)\\ \overline{w}(x,y)\\ \overline{\psi}_x(x,y)\\ \overline{\psi}_y(x,y)\end{Bmatrix} \tag{10}$$

In this study, the rectangular plate in Cartesian coordinates is mapped into a standard square. For numerical solution, the components of the vector $\mathbf{U}$ must be interpolated on the whole domain of the plate region. For in-plane components of the vector $\mathbf{U}$, the following simple polynomials are used:

$$\begin{cases}P_1(\theta^\alpha)=(1-\theta^\alpha),\quad P_2(\theta^\alpha)=(1+\theta^\alpha)\quad\alpha=1,2\\ P_k(\theta^\alpha)=(\theta^\alpha)^{k-3}(1-(\theta^\alpha)^2)\qquad k=3,4,...\end{cases} \tag{11}$$

Where θ^1 and θ^2 are natural coordinate systems and the functions P_1 and P_2 are used to satisfy in-plane boundary conditions. For interpolation of out-of-plane components, the following functions are used where H_k for $k=1,2,3,4$ are Hermitian shape functions that are used for satisfying out-of-plane boundary conditions.

$$\begin{cases}P_k(\theta^\alpha)=H_k(\theta^\alpha) & k=1,2,3,4\\ P_k(\theta^\alpha)=(1-(\theta^\alpha)^2)^{k-3} & k=5,6,...\end{cases} \tag{12}$$

Finally, two-dimensional interpolation functions can be written as:

$$n_i(\theta^1,\theta^2)=P_j(\theta^1)P_k(\theta^2) \tag{13}$$

Let

$$\mathbf{U}=\mathbf{N}\hat{\mathbf{X}} \tag{14}$$

Where $\hat{\mathbf{X}}$ is the generalized coordinate system and $\mathbf{N}$ is the shape function matrix. By this definition, $\mathbf{U}$ can be written as:

$$\mathbf{U}=\begin{Bmatrix}\overline{u}(x,y)\\ \overline{v}(x,y)\\ \overline{w}(x,y)\\ \overline{\psi}_x(x,y)\\ \overline{\psi}_y(x,y)\end{Bmatrix}=\begin{bmatrix}\mathbf{n}_{\overline{u}}&\mathbf{0}&\mathbf{0}&\mathbf{0}&\mathbf{0}\\ \mathbf{0}&\mathbf{n}_{\overline{v}}&\mathbf{0}&\mathbf{0}&\mathbf{0}\\ \mathbf{0}&\mathbf{0}&\mathbf{n}_{\overline{w}}&\mathbf{0}&\mathbf{0}\\ \mathbf{0}&\mathbf{0}&\mathbf{0}&\mathbf{n}_{\overline{\psi}_x}&\mathbf{0}\\ \mathbf{0}&\mathbf{0}&\mathbf{0}&\mathbf{0}&\mathbf{n}_{\overline{\psi}_y}\end{bmatrix}\begin{Bmatrix}\hat{\mathbf{X}}_{\overline{u}}\\ \hat{\mathbf{X}}_{\overline{v}}\\ \hat{\mathbf{X}}_{\overline{w}}\\ \hat{\mathbf{X}}_{\overline{\psi}_x}\\ \hat{\mathbf{X}}_{\overline{\psi}_y}\end{Bmatrix}=\begin{Bmatrix}\mathbf{N}_{\overline{u}}\\ \mathbf{N}_{\overline{v}}\\ \mathbf{N}_{\overline{w}}\\ \mathbf{N}_{\overline{\psi}_x}\\ \mathbf{N}_{\overline{\psi}_y}\end{Bmatrix}\hat{\mathbf{X}}=\mathbf{N}\hat{\mathbf{X}} \tag{15}$$

After formulation of components of displacement and rotation in accordance with hierarchical finite-element method, the mid-plane strains and curvatures expressed in Eq. (3) will encounter what follows:

$$\varepsilon_1^0 = \frac{\partial \mathbf{N}_{\bar{u}}}{\partial x}\hat{\mathbf{X}} + \frac{1}{2}\left(\frac{\partial \mathbf{N}_{\bar{w}}}{\partial x}\hat{\mathbf{X}}\right)^2,\quad \varepsilon_2^0 = \frac{\partial \mathbf{N}_{\bar{v}}}{\partial y}\hat{\mathbf{X}} + \frac{1}{2}\left(\frac{\partial \mathbf{N}_{\bar{w}}}{\partial y}\hat{\mathbf{X}}\right)^2$$

$$\varepsilon_4^0 = \mathbf{N}_{\bar{\psi}_y}\hat{\mathbf{X}} + \frac{\partial \mathbf{N}_{\bar{w}}}{\partial y}\hat{\mathbf{X}},\quad \varepsilon_5^0 = \mathbf{N}_{\bar{\psi}_x}\hat{\mathbf{X}} + \frac{\partial \mathbf{N}_{\bar{w}}}{\partial x}\hat{\mathbf{X}}$$

$$\varepsilon_6^0 = \frac{\partial \mathbf{N}_{\bar{u}}}{\partial y}\hat{\mathbf{X}} + \frac{\partial \mathbf{N}_{\bar{v}}}{\partial x}\hat{\mathbf{X}} + \frac{\partial \mathbf{N}_{\bar{w}}}{\partial x}\hat{\mathbf{X}}\frac{\partial \mathbf{N}_{\bar{w}}}{\partial y}\hat{\mathbf{X}}$$

$$\kappa_1^0 = \frac{\partial \mathbf{N}_{\bar{\psi}_x}}{\partial x}\hat{\mathbf{X}},\quad \kappa_2^0 = \frac{\partial \mathbf{N}_{\bar{\psi}_y}}{\partial y}\hat{\mathbf{X}},\quad \kappa_6^0 = \frac{\partial \mathbf{N}_{\bar{\psi}_x}}{\partial y}\hat{\mathbf{X}} + \frac{\partial \mathbf{N}_{\bar{\psi}_y}}{\partial x}\hat{\mathbf{X}}$$

$$\kappa_1^2 = -\frac{4}{3h^2}\left(\frac{\partial \mathbf{N}_{\bar{\psi}_x}}{\partial x}\hat{\mathbf{X}} + \frac{\partial^2 \mathbf{N}_{\bar{w}}}{\partial x^2}\hat{\mathbf{X}}\right),\quad \kappa_2^2 = -\frac{4}{3h^2}\left(\frac{\partial \mathbf{N}_{\bar{\psi}_y}}{\partial y}\hat{\mathbf{X}} + \frac{\partial^2 \mathbf{N}_{\bar{w}}}{\partial y^2}\hat{\mathbf{X}}\right)$$

$$\kappa_4^2 = -\frac{4}{h^2}\left(\mathbf{N}_{\bar{\psi}_y}\hat{\mathbf{X}} + \frac{\partial \mathbf{N}_{\bar{w}}}{\partial y}\hat{\mathbf{X}}\right),\quad \kappa_5^2 = -\frac{4}{h^2}\left(\mathbf{N}_{\bar{\psi}_x}\hat{\mathbf{X}} + \frac{\partial \mathbf{N}_{\bar{w}}}{\partial x}\hat{\mathbf{X}}\right)$$

$$\kappa_6^2 = -\frac{4}{3h^2}\left(\frac{\partial \mathbf{N}_{\bar{\psi}_x}}{\partial y}\hat{\mathbf{X}} + \frac{\partial \mathbf{N}_{\bar{\psi}_y}}{\partial x}\hat{\mathbf{X}} + 2\frac{\partial^2 \mathbf{N}_{\bar{w}}}{\partial x \partial y}\hat{\mathbf{X}}\right) \tag{16}$$

The weak form of the governing differential equations can be derived by using the principle of virtual work. The principle of virtual work in the present case yields:

$$\begin{aligned}&\int_\Omega \left(\overline{N}_i \delta\varepsilon_i^0 + \overline{M}_i \delta\kappa_i^0 + \overline{P}_i \delta\kappa_i^2 + \overline{Q}_1 \delta\varepsilon_5^0\right.\\ &\left. + \overline{Q}_2 \delta\varepsilon_4^0 + \overline{R}_1 \delta\kappa_5^2 + \overline{R}_2 \delta\kappa_4^2\right) dxdy \\ &- \int_\Omega \left(q(x,y)\,\delta w\right) dxdy = 0 \quad i = 1,2,6\end{aligned} \tag{17}$$

By substituting Eq. (16) into virtual work, Eq. (18) can be written as:

$$\begin{aligned}&\int_{-1}^{+1}\int_{-1}^{+1}\left[\overline{N}_1\left(\frac{\partial \mathbf{N}_{\bar{u}}}{\partial x} + \frac{\partial \mathbf{N}_{\bar{w}}}{\partial x}\hat{\mathbf{X}}\frac{\partial \mathbf{N}_{\bar{w}}}{\partial x}\right) + \overline{N}_2\left(\frac{\partial \mathbf{N}_{\bar{v}}}{\partial y} + \frac{\partial \mathbf{N}_{\bar{w}}}{\partial y}\hat{\mathbf{X}}\frac{\partial \mathbf{N}_{\bar{w}}}{\partial y}\right)\right.\\ &+ \overline{N}_6\left(\frac{\partial \mathbf{N}_{\bar{u}}}{\partial y} + \frac{\partial \mathbf{N}_{\bar{v}}}{\partial x} + \frac{\partial \mathbf{N}_{\bar{w}}}{\partial y}\hat{\mathbf{X}}\frac{\partial \mathbf{N}_{\bar{w}}}{\partial x} + \frac{\partial \mathbf{N}_{\bar{w}}}{\partial x}\hat{\mathbf{X}}\frac{\partial \mathbf{N}_{\bar{w}}}{\partial y}\right)\\ &+ \overline{M}_1\left(\frac{\partial \mathbf{N}_{\bar{\psi}_x}}{\partial x}\right) + \overline{M}_2\left(\frac{\partial \mathbf{N}_{\bar{\psi}_y}}{\partial y}\right) + \overline{M}_6\left(\frac{\partial \mathbf{N}_{\bar{\psi}_x}}{\partial y} + \frac{\partial \mathbf{N}_{\bar{\psi}_y}}{\partial x}\right)\\ &+ \overline{P}_1\left(-\frac{4}{3h^2}\left(\frac{\partial \mathbf{N}_{\bar{\psi}_x}}{\partial x} + \frac{\partial^2 \mathbf{N}_{\bar{w}}}{\partial x^2}\right)\right) + \overline{P}_2\left(-\frac{4}{3h^2}\left(\frac{\partial \mathbf{N}_{\bar{\psi}_y}}{\partial y} + \frac{\partial^2 \mathbf{N}_{\bar{w}}}{\partial y^2}\right)\right)\\ &+ \overline{P}_6\left(-\frac{4}{3h^2}\left(\frac{\partial \mathbf{N}_{\bar{\psi}_x}}{\partial y} + \frac{\partial \mathbf{N}_{\bar{\psi}_y}}{\partial x} + 2\frac{\partial^2 \mathbf{N}_{\bar{w}}}{\partial x \partial y}\right)\right) + \overline{Q}_1\left(\mathbf{N}_{\bar{\psi}_x} + \frac{\partial \mathbf{N}_{\bar{w}}}{\partial x}\right)\\ &+ \overline{Q}_2\left(\mathbf{N}_{\bar{\psi}_y} + \frac{\partial \mathbf{N}_{\bar{w}}}{\partial y}\right) + \overline{R}_1\left(-\frac{4}{h^2}\left(\mathbf{N}_{\bar{\psi}_x} + \frac{\partial \mathbf{N}_{\bar{w}}}{\partial x}\right)\right)\\ &\left.+ \overline{R}_2\left(-\frac{4}{h^2}\left(\mathbf{N}_{\bar{\psi}_y} + \frac{\partial \mathbf{N}_{\bar{w}}}{\partial y}\right)\right)\right]\delta\hat{\mathbf{X}}\left|\mathbf{J}(\theta^1,\theta^2)\right| d\theta^1 d\theta^2\\ &- \int_{-1}^{+1}\int_{-1}^{+1} q(\theta^1,\theta^2)\,\mathbf{N}_{\bar{w}}\delta\hat{\mathbf{X}}\left|\mathbf{J}(\theta^1,\theta^2)\right| d\,\theta^1 d\theta^2 = 0\end{aligned} \tag{18}$$

In Eq. (18), $\hat{\mathbf{X}}$ is an unknown matrix whose value is computed by means of Newton Raphson method.

4 NUMERICAL RESULTS AND DISCUSSIONS

In this study, the nonlinear analysis of FG plates was conducted for one type of ceramic and metal combination. The materials were considered to be Aluminium and Alumina. It is assumed that the upper surface is pure ceramic and the lower surface is pure metal. Since the Poisson's ratio varied in a small range it was assumed to be constant through the thickness of the FG plate. The material properties adopted here for obtaining the numerical results are:

Metal (Aluminium, AL): $E_m = 70\times10^9\ N/m^2$; $\nu = 0.3$.
Ceramic(Alumina, AL_2O_3): $E_c = 380\times10^9\ N/m^2$; $\nu = 0.3$.

In all cases the plate was subjected to a sinusoidally distributed load given by:

$$q(x,y) = q_0 \sin\frac{\pi x}{a}\sin\frac{\pi y}{b} \tag{19}$$

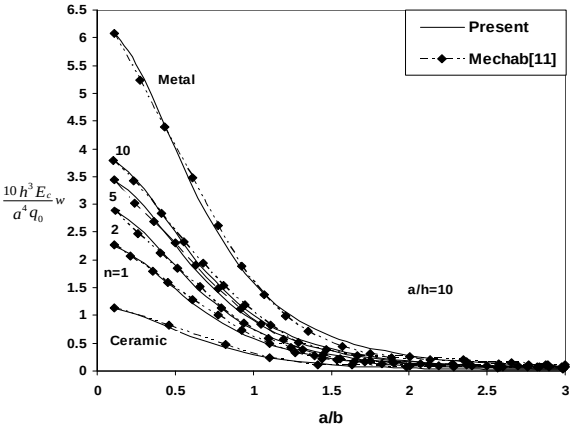

Fig. 2 Non-dimensionalized center deflection of SSSS FG plate versus aspect ratio

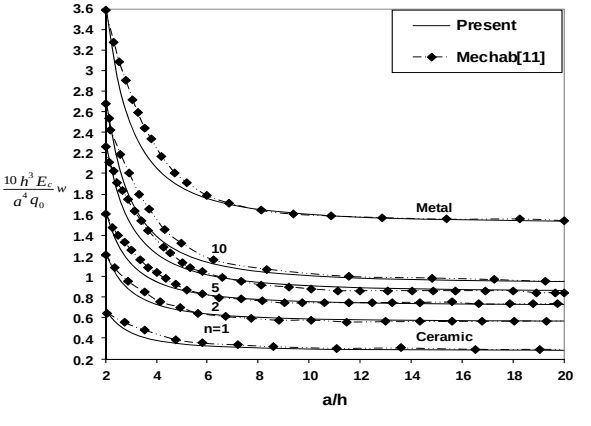

Fig. 3 Non-dimensionalized center deflection of SSSS FG square plate versus side-to-thickness ratio

Two different boundary conditions were considered as follows:
1- All edges simply supported (SSSS)
2- All edges clamped (CCCC)

In order to verify the accuracy of the presented method, hierarchical finite-element results of SSSS FG plates are compared with those of Matsunaga and Mechab available in literature [10], [11]. Figures 2 and 3 show non-dimensionalized center deflection of SSSS FG plate versus aspect ratio and side-to-thickness ratio for various volume fraction exponents (n).

It can be observed that the deflection is maximum for the fully metal plate and minimum for the fully ceramic plate, which can be attributed to the fact that the Young's modulus of ceramic is higher than that of metal. Deflection of FG plates is intermediate to that of the metallic and ceramic plates. Moreover, it is concluded from the figures that the deflection decreases by a rise in the aspect ratio, while it may be unchanged as the side-to-thickness ratio increases.

Figures 4 and 5 show through-the-thickness variations of non-dimensionalized normal stresses in x and y directions at the center point of SSSS FG plate for various side-to-thickness ratios and aspect ratios. It can be seen that the normal stresses are compressive throughout the lower half and tensile throughout the upper half of plate. As demonstrated, minimum value of zero for the normal stresses occurs at $z/h = 0.153$, which is independent of side-to-thickness ratio and aspect ratio.

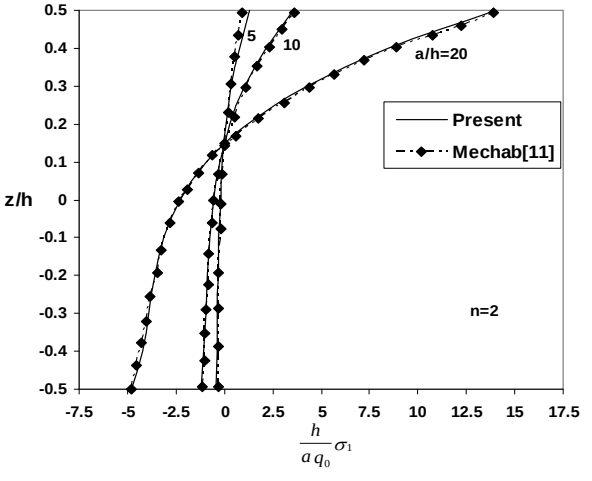

Fig. 4 Through-the-thickness variation of non-dimensionalized normal stress in x direction at the center point of SSSS FG square plate

The effect of volume fraction exponent (n) on non-dimensionalized normal stress in x direction of SSSS FG square plate is shown in Fig. 6.

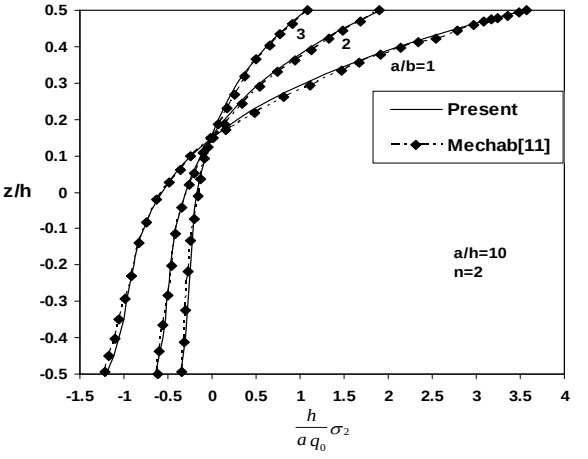

Fig. 5 Through-the-thickness variation of non-dimensionalized normal stress in y direction at the center point of SSSS FG plate

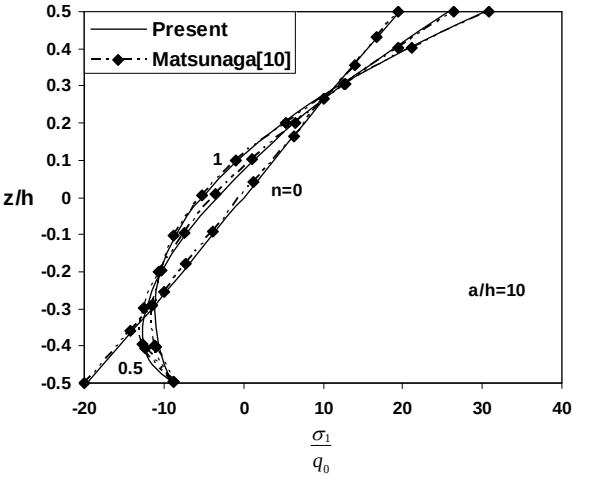

Fig. 6 Through-the-thickness variation of non-dimensionalized normal stress in x direction at the center point of SSSS FG square plate

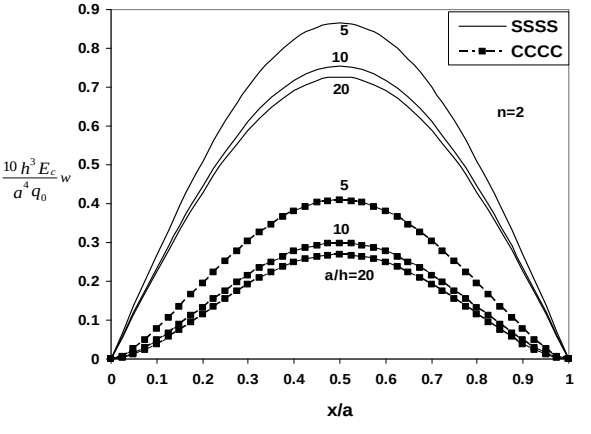

Fig. 7 Variation of non-dimensionalized deflection of SSSS and CCCC FG square plate along (x, b/2)

In Figs. 7 to 9 the nonlinear analysis is conducted for both fully simply supported and fully clamped FG square plates, and the results are compared with each other. The variation of non-dimensionalized deflection along $(x, b/2)$ for various side-to-thickness ratios is plotted in Fig. 7. Non-dimensionalized center deflection versus load for various volume fraction exponents (n) is shown in Fig. 8, and Fig. 9 depicts through-the-thickness variation of normal strain at the center point for different values of n. In this figure: $q_0 a^4 / E_m h^4 = 30$.

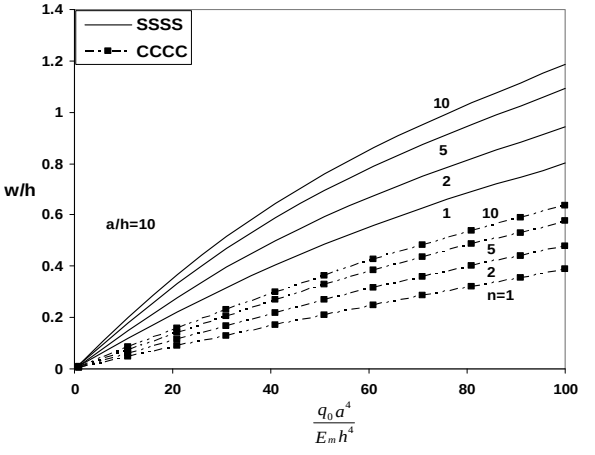

Fig. 8 Non-dimensionalized center deflection of SSSS and CCCC FG square plate versus load

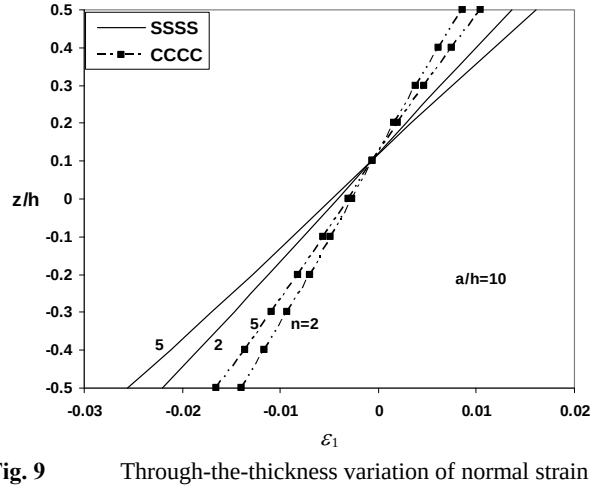

Fig. 9 Through-the-thickness variation of normal strain at the center point of SSSS and CCCC FG square plate

In the presented method, accurate results have been obtained even by few numbers of interpolation functions. In order to prove the idea, variation of center deflection of SSSS FG square plate versus numbers of interpolation functions are plotted in Fig. 10. It is observed that by using this method, there is no need to increase the numbers of interpolation functions.

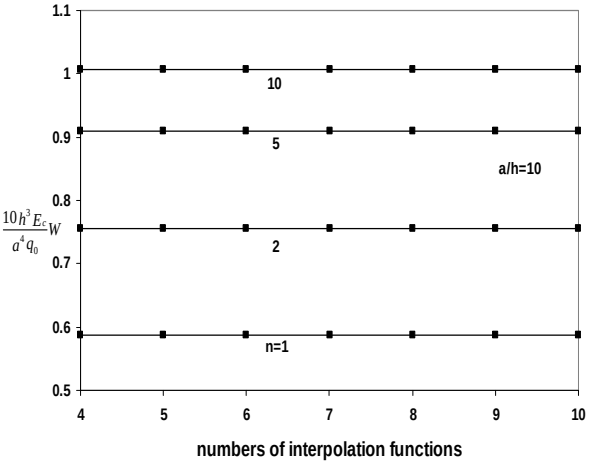

Fig. 10 Non-dimensionalized center deflection of SSSS FG square plate versus numbers of interpolation functions

5 CONCLUSION

Analysis of nonlinear bending behavior of thick FG plates subjected to sinusoidal loading for two kinds of boundary conditions has been carried out in the current study based on the third-order shear deformation plate theory and Von Kármán type non-linearity. The most important advantage of the employed numerical solution in this work is that the whole plate was considered as one element and the components of displacement field were interpolated over the entire domain, then a hierarchical finite-element scheme was developed. The method is computationally efficient and the numerical results are well in line with other solutions. Studying the effect of numbers of interpolation functions on the results revealed that reaching the accurate results is possible even by few numbers of interpolation functions. In general, it can be said that considering the whole plate as one element and using few numbers of interpolation functions save solution time.

REFERENCES

[1] Reddy, J. N., "A simple high-order theory for laminated composite plates", Journal of Applied Mechanics. Vol. 51, 1984, pp. 745-752.

[2] Reddy, J. N., "A refined nonlinear theory of plates with transverse shear deformation", Int. Journal of Solids and Structures, Vol. 20, 1984, pp. 881-896.

[3] Cheng, Z. -Q., Batra, R. C., "Deflection relationships between the homogenous kirchhoff plate theory and different functionally graded plate theories", Journal of Archives of Mechanics. Vol. 52, No.1, 2000, pp. 143-158.

[4] Woo, J., Meguid, S. A., "Nonlinear analysis of functionally graded plates and shallow shells", Int. Journal of Solids and Structures, Vol. 38, 2001, pp. 7409-7421.

[5] Ma, L. S., Wang, T. J., "Relationships between axisymmetric bending and buckling solutions of FGM circular plates based on third-order plate theory and classical plate theory", Int. Journal of Solids and Structures, Vol. 41, 2004, pp. 85-101.

[6] Chi, S. -H., Chung, Y. -L., "Mechanical behavior of functionally graded material plates under transverse load-part I: analysis," Int. Journal of Solids and Structures, Vol. 43, 2006, pp. 3657-3674.

[7] Nosier, A., Fallah, F., "Reformulation of mindlin–reissner governing equations of functionally graded circular plates", Int. Journal of Acta Mechanica, Vol. 198, 2008, pp. 209-233.

[8] Bo, Y., Hao-jiang, D., and Wei-qiu, C., "Elasticity solutions for functionally graded plates in cylindrical bending", Applied Mathematics and Mechanics (English Ed.), Vol. 29, No. 8, 2008, pp. 999-1004.

[9] Mian, A. M., Spencer, A. J. M., "Exact solutions for functionally graded and laminated elastic materials", Journal of Mechanics and Physics of Solids, Vol. 46 , No. 12, 1998, pp. 2283-2295.

[10] Matsunaga, H., "Stress analysis of functionally graded plates subjected to thermal and mechanical loadings", Journal of Composite Structures, Vol. 87, 2009, pp. 344-357.

[11] Mechab, I., Atmane, H. A., Tounsi, A., Belhadj, H. A., and Bedia, E. A. A., "A two-variable refined plate theory for the bending analysis of functionally graded plates", Int. Journal of Acta Mechanica, Vol. 26, 2010, pp. 941-949.

[12] Suresh Kumar, J., Sidda Reddy, B., and Eswara Reddy, C., "Nonlinear bending analysis of functionally graded plates using higher order theory", IJEST, Vol. 3, No. 4, 2011, pp. 3010-3022.

[13] Fereidoon, A., Asghardokht seyedmahalle, M., and Mohyeddin, A., "Bending analysis of thin functionally graded plates using generalized differential quadrature method", Int. Journal of Archive of Applied Mechanics. Vol. 81, 2011, pp. 1523-1539.

[14] Woodward, B., Kashtalyan, M., "Performance of functionally graded plates under localised transverse loading", Journal of Composite Structures, Vol. 94, 2012, pp. 2254-2262.

[15] Shen, H. -S., "Functionally graded materials: nonlinear analysis of plates and shells", New York: CRC Press, 2009, pp. 9-12.